ELSEVIER

Geomorphology 40 (2001) 291–309

GEOMORPHOLOGY

www.elsevier.com/locate/geomorph

Effects of large floods on sediment transport and reach morphology in the cobble-bed Sainte Marguerite River

B.C. Eaton [a,*], M.F. Lapointe [b,1]

[a] *Department of Geography, University of British Columbia, Vancouver, British Columbia, Canada*
[b] *Department of Geography, McGill University, Montreal, Quebec, Canada*

Received 20 September 2000; received in revised form 12 February 2001; accepted 14 February 2001

Abstract

Sediment transport rates were estimated for two flood events on the cobble-bed Sainte Marguerite River in the Saguenay region, Canada. Morphologic methods were used to derive one set of estimates, and a combination of the Meyer-Peter and Muller equation with a dimensionless sediment transport ratio (after Dietrich et al. [Nature 340 (1989) 215]) was used to derive another set of estimates. Both sets of estimates give consistent results for the first event (which had a decade-scale return period), and for the second event (which was the largest flood on record and had a century-scale return period). The transport occurring during the second event was an order of magnitude greater than that occurring during the first event: despite this disparity in the transport intensity of the two events, the channel morphology remained qualitatively similar. The observed degree of channel stability is attributed to a change of channel pattern and the initiation of bed degradation following channel rectification in the 1960s.

Keywords: Flood; Channel morphology; Sediment transport; Flood plain

1. Introduction

The literature pertaining to the geomorphic impacts of rare flood events is, by definition, sparse. Given the nature of such events, the data are usually insufficient to accurately quantify the geomorphic impacts because there is little pre-flood information. Assessment of channel pattern changes from air photos is a common practice (Desloges and Church, 1992), as is reliance upon previously existing cross-sectional information (Ritter, 1974; Miller, 1990). However, these techniques are often inadequate to determine the vertical component of change, the extent and precise pattern of planform adjustment, or changes in the bed sediment caliber. That such data is often the best available information on rare floods is due to the practical impossibility of designing a research program to study them: nature simply does not provide high return period floods at predictable intervals.

From the data available, however, several typical geomorphic responses to large floods are consistently reported. The most obvious adjustment is a widening of the channel, often by two- or threefold. Such widening is often observed in arid and/or alpine environments, where there is sparse riparian vegetation (Huckleberry, 1994; Warburton, 1994).

* Corresponding author. Fax: +1-604-822-6150.
E-mail addresses: beaton@geog.ubc.ca (B.C. Eaton), lapointe@felix.geog.mcgill.ca (M.F. Lapointe).
[1] Fax: +1-514-398-7437.

0169-555X/01/$ - see front matter
PII: S0169-555X(01)00056-3

This widening is often associated with a change in channel pattern from a single thread meander to a braided channel (Desloges and Church, 1992; Warburton, 1994). Less extreme adjustments may also occur during large floods, but go undetected for lack of adequate pre-flood data. The morphologic response of stream channels to large floods involve larger-than-average volumes of sediment transport. Arguably the most appropriate variable for characterizing the size of a rare event (when discussing morphologic change) is the total bed material transport occurring during that event, rather than the peak discharge or total volume of flood-related runoff.

Many sediment transport equations based on shear stress or some equivalent measure of fluid force exist, though a generally applicable equation has not yet been developed (Gomez and Church, 1989; Reid and Frostick, 1994). These are easily used to reconstruct sediment transport rates during large floods, but their poor performance when applied to data sets not used for development of the predictive relation (Gomez and Church, 1989) makes the resulting transport estimates suspect. Alternatively, event-scale transport rates may be calculated from net changes in sediment storage within the channel (Popov, 1962; Hubbel, 1964; Neill, 1971, 1987; Carson and Griffiths, 1989; Lane et al., 1995; Martin and Church, 1995; Ashmore and Church, 1998; Ham and Church, 2000). This alternate approach has been called the "morphologic" (or "inverse") method for estimating bed material transport; it requires that detailed topographic information is available prior to and following the flood event, which is not usually the case.

By definition, morphologic methods are limited to estimates of the transport of the bed material fraction only; sediment in transport that does not interact with the bed cannot be assessed using this approach. Furthermore, these methods yield minimum estimates of bed material flux, because neither the net throughput of sediment nor the volume of compensating scour and fill at the same location (hence resulting in no net bed change), can be estimated, without additional data (Ashmore and Church, 1998). Sediment throughput can be accounted for when mobile bed sediments have been directly sampled, or when local throughput is known to be zero (downstream of a lake or dam, for example). Scour and compensating fill can be accounted for when ancillary information is available, such as that obtained using scour chains (see Hassan, 1990; Haschenburger and Church, 1998).

The objectives of this study are to: (i) estimate sediment transport during two flood events using morphologic methods and a combination of the Meyer-Peter and Muller equation with a dimensionless sediment transport ratio (after Dietrich et al., 1989), and (ii) determine the morphologic response to the two flood events.

2. Study area

The study reach is in the upper part of the Sainte Marguerite River, a cobble-bed river in the Saguenay region of Quebec. The drainage basin area upstream of the reach is 285 km^2. The study reach is part of an 8-km section of the Sainte Marguerite River that was rectified in the early 1960s during construction of Highway 172; all of the natural meanders were bypassed by man-made channels cut through the neck of the meanders. As a result, channel sinuosity decreased from 1.9 prior to channelization to 1.2 following it. Assuming that the vertical drop over the rectified section of channel was initially unchanged, this produced nearly a 50% increase in the channel gradient after rectification. Recent work has shown that, over the past 4 decades there has been 0.5–1.0 m of bed degradation in the vicinity of the study reach as a result of this rectification (Talbot and Lapointe, in review/a,b). While some parts of the rectified section of Sainte Marguerite River have undergone rapid and extensive planimetric changes in an attempt to reestablish a higher sinuosity, a comparison of the extant study reach morphology with that evident on aerial photos taken immediately after rectification reveals that the study site has not undergone significant lateral adjustment since rectification, and that the location of the primary morphologic elements has not changed (Eaton, 1996), despite significant bed degradation.

Fig. 1 shows the study reach and its upstream extension, indicating the location of the channel bars and other key features of the reach. While a sinuous meander has grown since rectification just upstream, the study reach is relatively straight, encompassing two lateral bars and the head of a third lateral bar.

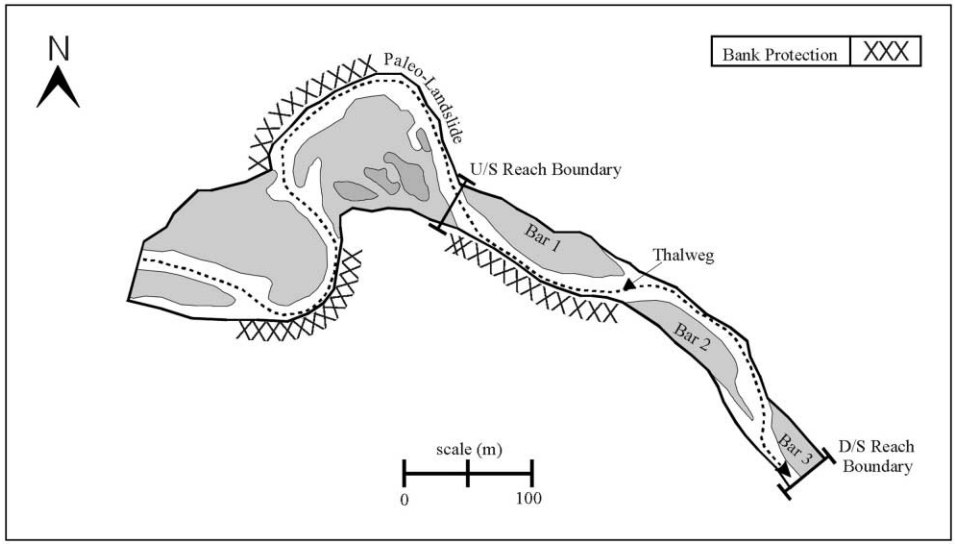

Fig. 1. Study reach within the channelized section of the Sainte Marguerite River in the Saguenay region of Quebec, Canada. Meander rectification occurred during construction of Highway 178 in the 1960s. The riprap bank protection shown was installed in 1993.

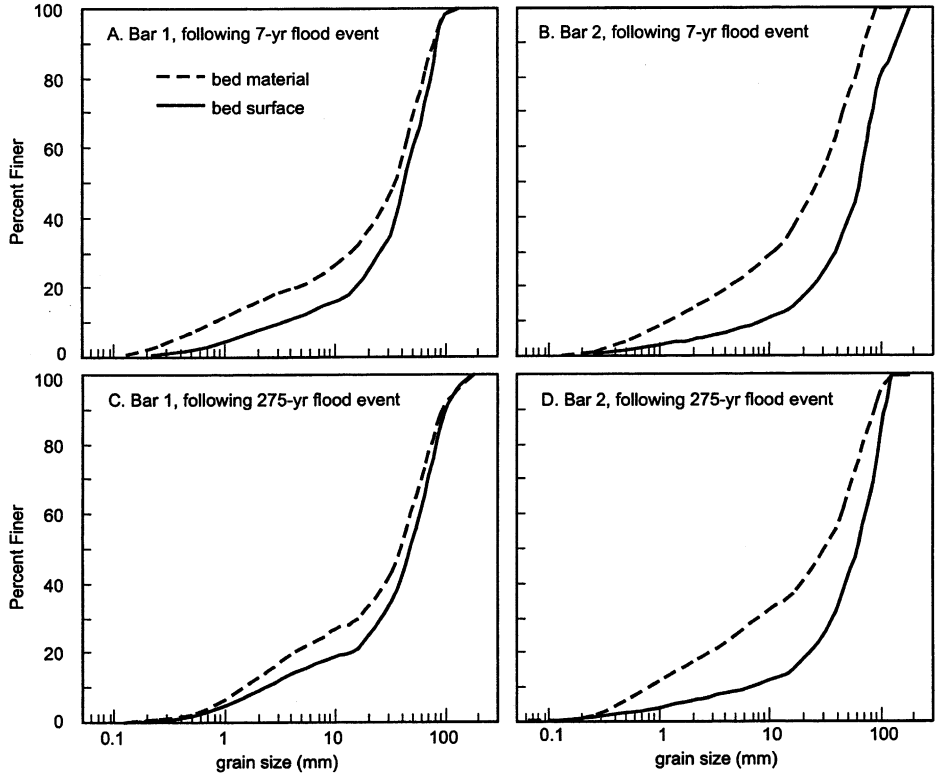

Fig. 2. Grain size distributions for the bed surface and the underlying bed material are presented for bars 1 and 2. Samples were taken following both the 7- and 275-year flood events. Sample locations are shown in Fig. 4.

The cutbank opposite the upstream-most bar (bar 1) was protected in 1993 by riprap up to about 1 m in diameter. The meanders immediately upstream of the reach are associated with two complex point bars, which store large amounts of sediment. The cutbanks of these bars have also been protected with riprap, and a bank segment is naturally armored by large clasts input by an ancient landslide.

The reach is 352 m long, has a cobble-gravel bed with a thalweg gradient of 0.0028 m/m, and is 38 m wide (at bankfull), on average. Bulk samples of the surface grain size distribution at the bar heads (representing the coarsest bed material actively transported) are presented in Fig. 2. These samples give an average D_{50} of 55 mm and an average D_{90} of 115 mm (sample size was approximately 125 kg, giving a precision for the size percentiles between 1% and 2%, after Church et al., 1987). The mean annual peak daily discharge at the study reach is estimated to be about 90 $m^3\ s^{-1}$.

3. Flood conditions in 1996

There is no historical flood record on the mainstem of the Sainte Marguerite River with which to recreate the flow conditions at the study site during the flood events on May 16, 1996 or July 20, 1996. However, the maximum water elevation on May 16, 1996 (the peak of the freshet) was observed and recorded in the field at the upstream boundary. Also, an apparent high water line on a sandy bank near the downstream boundary was recorded on May 27, 1996 following recession of the flood, which was consistent with the upstream high water level and the water surface slope surveyed in the field at a flow roughly 1/3 of the estimated mean annual maximum flow (36 $m^3\ s^{-1}$). On July 22, 1996 (2 days after the 275-year peak flow), maximum stage indicators were observed and recorded at the upstream boundary; no markers were evident near the downstream reach boundary. Given this information, average hydraulic radii were calculated for both the events and slope-area estimates of the flood discharges were computed. Manning's equation was used to produce estimates of the average velocity based on the water surface slope data, and applied over the reach average cross-sectional area to produce a discharge estimate. Manning's n estimates were based on grain size data at the bar heads using Strickler's law. The resulting discharge estimates are presented in Table 1.

Table 1
Estimated flow conditions for 1996 flood peaks at the study site

Parameter	May 16, 1996 flood event	July 20, 1996 flood event
Discharge ($m^3\ s^{-1}$)	143 ± 29	246 ± 46
Estimated return period (yr)	5.6–7.9	168–398
Reach mean shear stress ($N\ m^{-2}$)	45 ± 7	61 ± 8
Reach mean stream power ($W\ m^{-2}$)	104 ± 41	178 ± 69

Flow during the smaller event on May 16, 1996 was primarily confined within the channel, though overbank flooding did occur several kilometers downstream where the river was not so deeply incised. The river stage exceeded the bank top during the larger event on July 20, 1996; however, accurate estimates of the overbank discharge were not possible, because (i) the precise flood water elevation was evident only near the upstream end of the reach, not throughout the reach, and (ii) the dense vegetation on the flood plain make estimating appropriate values of Manning's n difficult. Peak discharge estimates in Table 1 do not account for any flow occurring outside the channel on the flood plain during the July 20, 1996 event. Note, however, that the overbank flooding did not do any geomorphic work, except for local erosion of unvegetated road surfaces, and can therefore be ignored for the purposes of this analysis: that is, the discharges in Table 1 are effective discharges.

The return period of these two events was estimated based on the records from a gauge that has been in operation since 1974 on the North East Branch of Sainte Marguerite River. The gauge is located near the confluence with the mainstem, which is downstream of the study reach. The drainage area of the North East Branch is physiographically representative of the drainage area upstream of the study reach; and was subject to the same hydrologic conditions that generated both flood events. The first flood event (peak $Q = 143\ m^3\ s^{-1}$) occurred during the

snowmelt-fed spring freshet; it peaked on May 16, 1996, and had an estimated return period of about 7 years (Table 1). The second flood (peak $Q = 246$ m^3 s^{-1}) event was triggered by exceptional frontal precipitation on July 20, 1996; it was the largest flood in a 22-year record, and had a return period of about 275 year (Table 1).

Reach-average shear stress and stream power within the bankfull channel were estimated using the usual one-dimensional uniform flow approximations:

$$\tau_o = \rho g R S_w \quad (1)$$

$$\omega = \rho g Q S_w / w \quad (2)$$

where τ_o is the reach-average shear stress (N m^{-2}), ρ is the density of water (kg m^{-3}), g is the acceleration of gravity (m s^{-2}), R is the hydraulic radius (m), S_w is the water surface slope (m/m), ω is the average specific stream power (W m^{-2}) and w is the water surface width (m) corresponding to the discharge, Q (m^3 s^{-1}). These estimates are presented in Table 1.

The errors presented in Table 1 were derived based on the uncertainty of the estimates of hydraulic radius, water surface slope, cross-sectional area and Manning's n. Uncertainties in peak stage estimates were negligible compared to the other sources of error in the slope-area calculations. Since entry and exit cross-sectional areas were approximately equal, no velocity head correction was made and the energy slope was assumed to be identical to the water surface slope.

4. Methods

4.1. Digital elevation models of pre- and post-flood channel

The reach morphology was surveyed three times using a Total Station. These surveys bracket the two flood events described above. The density of the survey data varied from 1 point per 5 m^2 to 1 point per 9 m^2, giving a mean point spacing of 2.1–3.0 m. Within a given set of survey data points, point spacing varied from < 1 to about 5 m, depending on the topographic complexity. Digital elevation models with a grid cell size of 10 cm, and vertical resolution of 1 cm were constructed for the three survey floods, using an inverse-distance weighting procedure. Uncertainties in the survey measurements were less than 1 cm.

4.2. Transport estimates using morphologic methods

The amount of bed material transported during these two flood events was estimated using morphologic methods because: (i) the short duration of the spring snowmelt event, and regional road closures due to flooding during the July 1996 event made it very difficult to be present during the peaks of the event; and (ii) bed material transport in cobble bed streams is extremely difficult to measure accurately at the event scale.

The first morphological method relies on establishing a sediment budget by integrating a general statement of continuity of mass across the channel, yielding a one-dimensional finite difference equation for changes along the channel (Ashmore and Church, 1998):

$$(1 - p)\Delta V + (Q_{bo} - Q_{bi})\Delta t = 0 \quad (3)$$

where p is the porosity; ΔV is net volumetric change (m^3) in storage of sediment within a given zone, ($\Delta V = V_i - V_o$ where V_i is the volumetric sediment input to the zone and V_o is the volumetric sediment output from it); Q_b is the cross-sectional volumetric sediment transport rate (m^3 s^{-1}) (Q_{bi} is the transport rate at the upstream boundary of the reach and Q_{bo} is the transport rate at the downstream boundary); and Δt is the event duration. These estimates were then transformed to estimates of the bulk transport rate by assuming a porosity of 0.29 (after Carling and Reader, 1982) and a constant particle density of 2650 kg m^{-3}: this corresponds to a bulk density of 1890 kg m^{-3} for the bed material. The bulk transport rate per unit width (i_b) is reported in kg m^{-1} event^{-1} and the total bulk transport rate (I_b) is reported in kg event^{-1}.

Eq. (3) can be used to calculate the change in sediment transport within a reach based on storage changes (Ashmore and Church, 1998), given an input or output sediment transport rate. In the absence of such direct measurements, a zero transport condition must be assumed at a given point, the validity of which can be assessed based on comparisons with

other methods (e.g., Goff and Ashmore, 1994). Any component that is carried through the reach without interacting with the morphology is not recorded. Volumetric sediment transport (Q_b) into and out of each segment was calculated by specifying a zero transport condition at an arbitrary location such that no negative (and physically impossible) transport rates result. This assumption is necessary because no input or output sediment transport rate was available nor was any physically based zero transport location; this approach is reasonable, and has several precedents in the literature (Martin and Church, 1995; Wathen and Hoey, 1998; Ham and Church, 2000). By applying this method to 14 zones in the study reach—which are shown in Fig. 3—both a reach-average I_b and a peak within-reach I_b have been calculated for both flood events.

Other morphologic methods used to estimate I_b during these two events are based on the *step length* for gravel transport (Neill, 1971, 1987; Carson and Griffiths, 1989; Goff and Ashmore, 1994; Lane et al., 1995; Ashmore and Church, 1998). The most intuitive method of calculating i_b is by identifying a discrete zone of erosion and pairing it to a zone of deposition downstream (Ashmore and Church, 1998). Transport rates calculated using this *paired erosion/deposition* method apply only to the bed between corresponding erosion and deposition zones, and represent peak within-reach values of i_b, not reach-average values.

Zone	Total Area (m^2)	Changes in net sediment storage			
		7-yr Flood		275-yr Flood	
		(m^3)	(cm/m^2)	(m^3)	(cm/m^2)
all	**35662.70**	**-277.22**	**-0.8**	**77.50**	**0.2**
1	1417.72	-45.53	-3.2	-56.28	-4.0
2	1570.96	-67.01	-4.3	135.11	8.6
3	1406.17	-22.76	-1.6	159.69	11.4
4	1020.63	17.31	1.7	67.11	6.6
5	922.42	81.75	8.9	18.29	2.0
6	940.97	-30.58	-3.2	-29.79	-3.2
7	850.24	-15.16	-1.8	-126.41	-14.9
8	1150.33	31.01	2.7	-90.97	-7.9
9	973.96	28.76	3.0	-15.44	-1.6
10	1069.33	-108.12	-10.1	-37.23	-3.5
11	999.61	5.01	0.5	97.52	9.8
12	843.82	-68.30	-8.1	232.21	27.5
13	874.01	-103.06	-11.8	14.62	1.7
14	1063.09	19.49	1.8	-290.93	-27.4

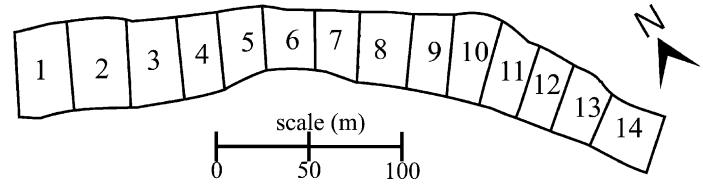

Fig. 3. Channel zones used in the sediment budget. Individual zone areas are indicated, as are the net changes in volume of stored sediment resulting from the 7- and 275-year flood events. Changes in stored volume are expressed in m^3 and in cm/m^2. Net deposition is indicated by (+) and net erosion by (−).

A more general method using the step length involves applying a typical step length to the *total erosion* measured within the reach. The equation summarizing this total erosion method, as presented in Ashmore and Church (1998), is

$$I_b = \rho_s V_e (L_s / L_r) / t \quad (4)$$

where I_b is the bulk sediment transport rate (kg s^{-1}), ρ_s is the bulk density of gravel (taken to be 1890 kg m^{-3}), V_e is the total volume of erosion (m^3), L_s is the step length (m), L_r is the length of the reach (m) over which V_e was determined, and t is the event duration. Step length was estimated from the distance between the centroids of erosion and deposition for erosion/deposition pairs in the main channel. Because no convincing pairs of erosion and deposition were identified for the 275-year event, a functional relation between excess stream power and the virtual transport rate in a wide range of fluvial environments presented by Hassan et al. (1992) was used to estimate step length for this event.

The precision with which net changes in stored sediment can be determined is a function of the density of the survey data, the lateral and vertical extent of the net erosion or deposition, and the complexity of the channel morphology. Based on paired zones of erosion and deposition (discussed in Section 5.2), there is typically on the order of about 4% uncertainty in erosion and deposition volume estimates. Uncertainty in bulk density derives primarily from variations in porosity (Carling and Reader, 1982), not from variations in particle density: it is conservatively estimated to be on the order of $\pm 17\%$, based on the range of porosity values reported by Graton and Fraser (1935). Provided that all the assumptions made in generating the morphologic method sediment transport estimates above are true, the uncertainty in the estimates of I_b is likely on the order of 18%, and is primarily a function of uncertainty in the bulk density. In reality, the primary source of uncertainty in these estimates likely derives from the necessary assumptions, particularly regarding the absence of sediment throughput and compensating scour and fill; there is no obvious way to quantify uncertainty deriving from these assumptions.

4.3. Transport estimates using the dimensionless sediment transport ratio (q^*)

Another set of transport rate estimates was made based on fluid force and the estimated degree of sediment supply limitation. A dimensionless *sediment transport ratio* (q^*)—based on the observed degree of bed armoring within the reach (after Dietrich et al., 1989)—has been combined with estimates of potential sediment transport rate (I'_b). Thus:

$$I_b = (q^*)(I'_b) \quad (5)$$

where *potential sediment transport rate* (I'_b) is the sediment transport that would occur if transport were not limited by sediment supply. I'_b was estimated via the Meyer-Peter and Muller equation, using as the characteristic sediment size the D_{50} of the subsurface material, which reflects the bed material load. Bed textures were relatively uniform (except very close to the banks) along section A–A' and were assumed to correspond to those at the head of bar 1 ($D_{50} = 39$ mm, see Fig. 2). The Meyer-Peter and Muller equation was initially developed based on flume experiments, and has been used for steep cobble and gravel bed streams (e.g., Church et al., 1998).

Rather than applying the Meyer-Peter and Muller equation to cross-sectional average flow conditions —which would not necessarily reflect the cross-sectional average transport, due the potentially limited spatial extent of gravel transport on the bed (Carson and Griffiths, 1987)—the potential sediment transport per unit of channel width, i'_b was estimated based on local flow conditions. Shear stress was estimated at 1-m increments across the channel at cross-section A–A′ (Fig. 4), using the approximation:

$$\tau_o = \rho g Y_i S w \quad (6)$$

where Y_i is the local water depth at the ith point on the cross-section (m). This first approximation is reasonable for straight, wide channels with gradually varying depths across the section and with uniform flow downstream. Cross-section A–A′ (width:depth ratio = 38) fits these conditions better than other possible cross-sections in the reach. It also remained

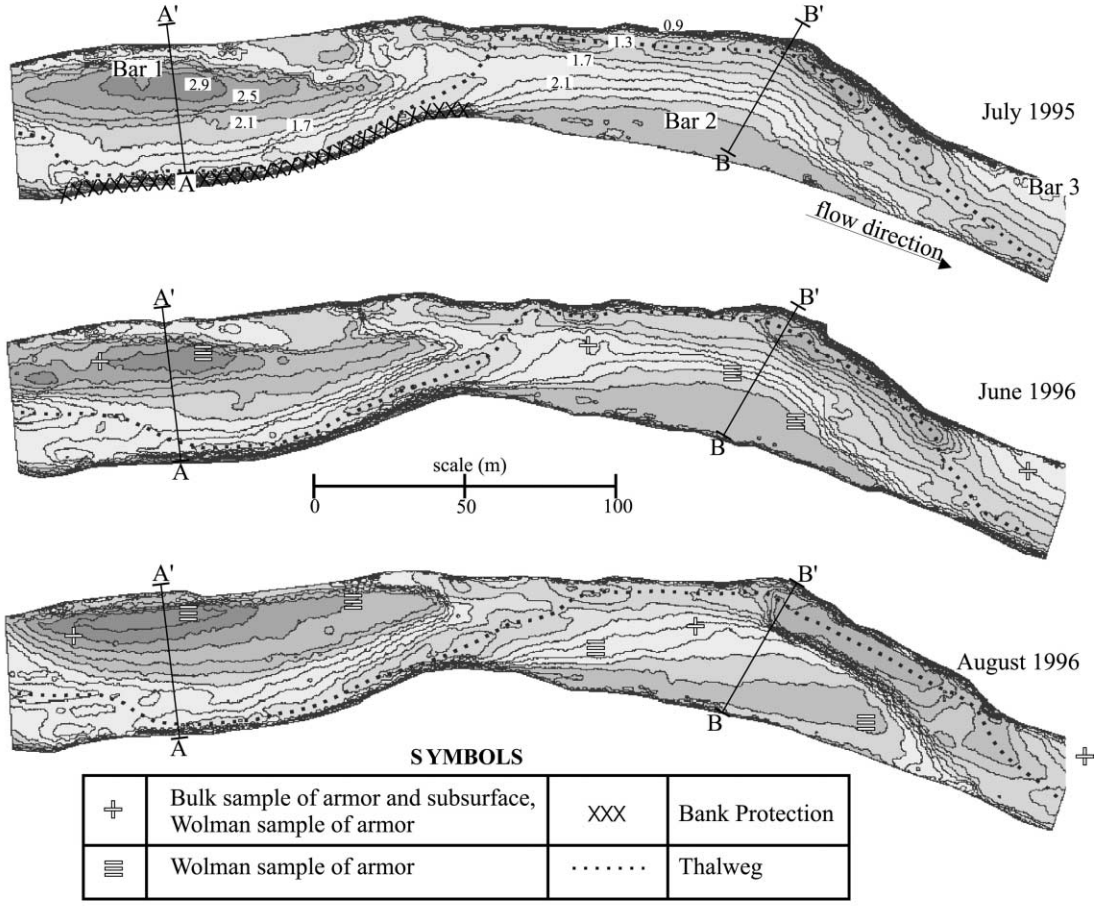

Fig. 4. Digital elevation models for the three surveys bracketing sediment transport events peaking on May 16, 1996, and July 20, 1996. The extent of the bank protection is shown on the July 1995 DEM, as are contour labels. The datum of 0.0 m corresponds to an elevation of 125.9 m above mean sea level. The contour interval is 0.2 m.

relatively stable throughout the course of both floods, in large part due to protection along the right bank (Fig. 1). While there has been laterally extensive but vertically limited net erosion on the face of bar 1 (refer to Fig. 5, a map of net erosion and deposition), the dominant change here was infilling of the secondary channel during the 275-year event, presumably during flood recession. Also, the best physical indicators of the peak water levels for both flood events were located just upstream of cross-section A–A′, and water levels are known most accurately here.

The shear stress field—$\tau_o(x)$, where x is the cross-channel position—was used to generate a potential sediment transport field $i'_b(x)$, in kg m^{-1} event^{-1}. $i'_b(x)$ was then integrated across the channel to yield the cross-sectional potential transport rate (I'_b in kg event^{-1}). This lateral integration provides more accurate estimates (Carson and Griffiths, 1987) and resolves the spatial distribution of i'_b across the channel at A–A′.

The temporal changes in I'_b over the course of the extreme July 1996 flood of multi-day duration have also been considered. The hydrograph for this event

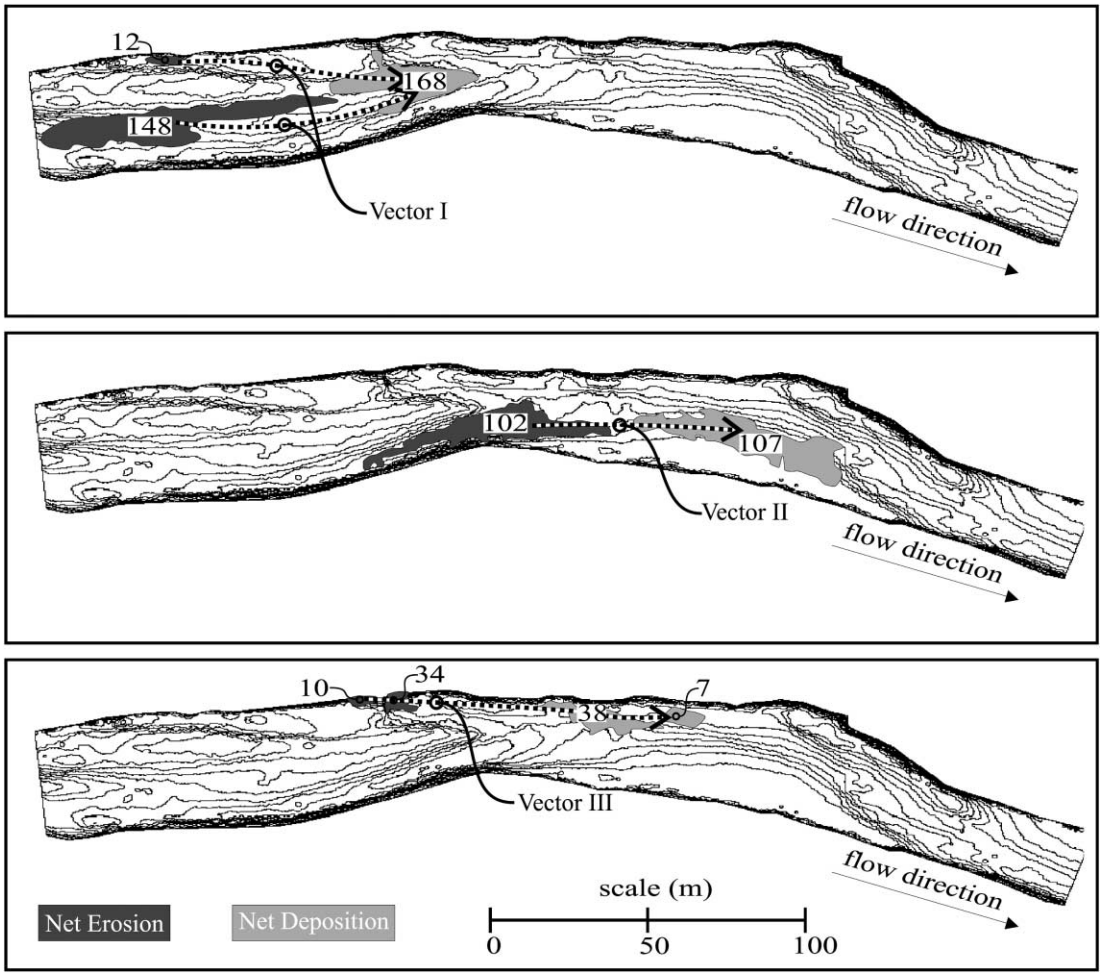

Fig. 5. Paired areas of net erosion and net deposition resulting from the 7-year flood event. The volumes of erosion and deposition are provided for each pair in m^3. The inferred sediment transport path between the pairs is shown, and each transport vector is labeled. All information overlies the contours from the June 1996 DEM.

as recorded at the existing gauge on the North East Branch was used to reconstruct a flood hydrograph for the study reach (Fig. 6). Using the recorded daily discharges, a hydrograph of discharge on the ith day (Q_i) normalized by the mean annual maximum daily discharge (Q_2) was generated for July 19–25, 1996 (Fig. 6). By equating the reconstructed peak discharge at the study reach (246 $m^3\ s^{-1}$) with the normalized discharge (Q_i/Q_2) observed on July 20, 1996, discharge estimates (in $m^3\ s^{-1}$) have been generated for July 19–25, 1996. These estimates where then used to reconstruct the cross-sectional shear stress distribution at cross-section A–A′, using Manning's equation (assuming a constant roughness value), the water surface elevation, and associated hydraulic radius.

The observed peak water level on May 16, 1996, was used to estimate the $i'_b(x)$ field at A–A′. The gauging station on the east branch of the Sainte Marguerite was out of commission between May 13 and July 16, 1996, and a flood hydrograph for the 7-year event could not be reconstructed. However, by using the calculated virtual transport rate (after Hassan et al., 1992) and the known step length for

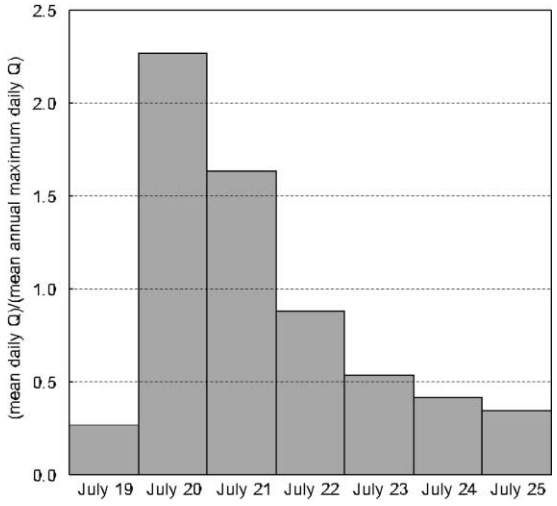

Fig. 6. Flood hydrograph for July 19–25, 1996, at the hydrometric gauge located on the North East Branch of the Sainte Marguerite River. The daily discharge values have been normalized by the mean annual maximum daily discharge, which is 268 $m^3\ s^{-1}$ for the North East Branch.

this event, transport is estimated to have persisted for 48 h. I'_b was derived by integrating $i'_b(x)$ for May 16, 1996 across the channel, and assuming and event duration of 2 days.

The dimensionless sediment transport ratio (q^*) reflects the fact that streams develop increasingly coarse surface layers in response to decreasing rates of sediment supply (for fixed increments of sediment transport capacity based on the sub-pavement texture). As evident in Eq. (5), the dimensionless sediment transport ratio is simply the ratio of actual transport to the potential sediment transport (I_b/I'_b). The equation presented in Dietrich et al. (1989) for calculating q^* based on the observed degree of bed armoring under conditions of limited sediment supply is:

$$q^* = \left(\frac{\frac{\tau_b}{\tau_{cl}} - \alpha\left(\frac{D_{50s}}{D_{501}}\right)}{\frac{\tau_b}{\tau_{cl}} - 1} \right)^{1.5} \quad (7)$$

where τ_b is the boundary shear stress imposed by a given set of flow conditions (N m^{-2}), τ_{cl} is the critical shear stress for the subsurface (or the bed load), α is a parameter equal to 1 for gravel with a uniform bulk density, D_{50s} is the median particle size (m) of the surface, and D_{501} is the median particle size (m) of the subsurface/bed load. A q^* value close to 0 implies that there is no sediment supply (the bed is tending toward a static armor), and a q^* value near 1 implies that sediment transport is equivalent to the sediment supply.

Reach sedimentology has been characterized by bulk samples (Church et al., 1987) of the bed material and Wolman samples of the bed surface (Fig. 2). The location of the sediment samples is shown in Fig. 4. Bulk samples were about 200 kg; the estimated precision for the size percentiles is between 1% and 2% (Church et al., 1987). Samples were taken immediately after the 7-year flood event and again after the 275-year event. The degree of armoring produced by each flood event is known, and one can infer the degree to which sediment transport during each event was supply limited (Dietrich et al., 1989).

To clarify the presentation of results and subsequent discussion, transport rates based on changes in channel morphology are referred to using the notation $i_b(\mathrm{d}x, \mathrm{d}y, \mathrm{d}z)$ and $I_b(\mathrm{d}x, \mathrm{d}y, \mathrm{d}z)$. Transport rates based I'_b and q^* are referred to using the notation $I_b(q^*, I'_b)$.

5. Results

5.1. Patterns of channel change

Maps of the reach morphology generated using the digital elevation models for the three surveys are presented in Fig. 4. The longitudinal profile following the thalweg and two representative cross-sectional profiles through bars 1 and 2 have been extracted from each digital elevation model and are presented in Figs. 7 and 8. Fig. 7 presents the longitudinal and cross-sectional profiles before and after the 7-year flood event, and Fig. 8 presents the profiles before and after the 275-year event.

The patterns of morphologic response to the 7- and 275-year floods are clearly evident upon comparison of the bar morphology before and after each flood event (Fig. 4). The morphologic response to both flood events is qualitatively similar. Bar 1 has progressed downstream (primarily during the 7-year

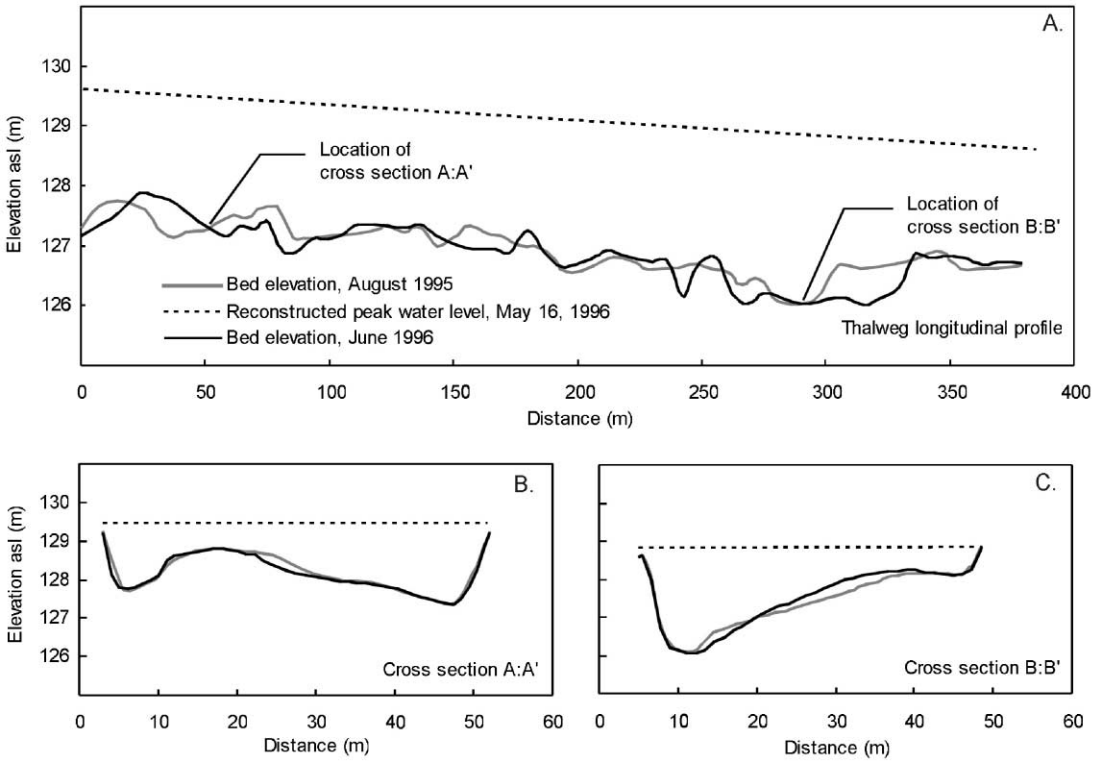

Fig. 7. Longitudinal (A) and cross-sectional (B and C) profiles of the study reach before and after the 7-year flood event. The cross-section locations are indicated in Fig. 4. The longitudinal profile follows the thalweg as shown on the July 1995 DEM. The reconstructed peak water elevation is shown on all profiles.

flood) and towards the left bank (during the 275-year flood). This bar has responded to sediment supplied from upstream by growing downstream and filling in the secondary channel behind the bar crest. It has not advanced towards the right bank (which is the normal pattern of bar growth) because of the riprap bank protection, which prevents the occurrence of cutbank retreat necessary to accommodate lateral accretion on the bar. Cross-section A–A′ through bar 1 clearly illustrates the altered pattern of bar growth (Figs. 7B and 8B). In fact, sediment previously deposited on the face of bar 1 (towards the thalweg) was eroded during the 7-year flood. Bar 2 has advanced towards the left bank (cross-section B–B′, Figs. 7C and 8C). The left bank opposite bar 2 is unprotected and has retreated, especially during the 275-year flood event. Bar 2 it has also migrated downstream; while the downstream migration is most pronounced in response to the 275-year flood, it is also detectable in response to the 7-year flood along the downstream edge of the bar.

Prior to the 7-year flood, a prominent diagonal riffle existed between bar 1 and 2. This riffle degraded during both the 7- and 275-year floods as a result of bar 2 moving down-channel with respect to bar 1 (Fig. 4, at 160 m, Fig. 7A, and at 180 m, Fig. 8A). Normally, one would expect that—in the case of migrating lateral bars—morphologic elements would migrate downstream coherently. In this case, the bank protection has accommodated some movement of bar 1 downstream (during the 7-year flood), but its position has subsequently become fixed. Bar 2 is not constrained by bank protection and has continued to migrate downstream, resulting in the degradation of the diagonal riffle between these two bars. Downstream, a new riffle crest has developed be-

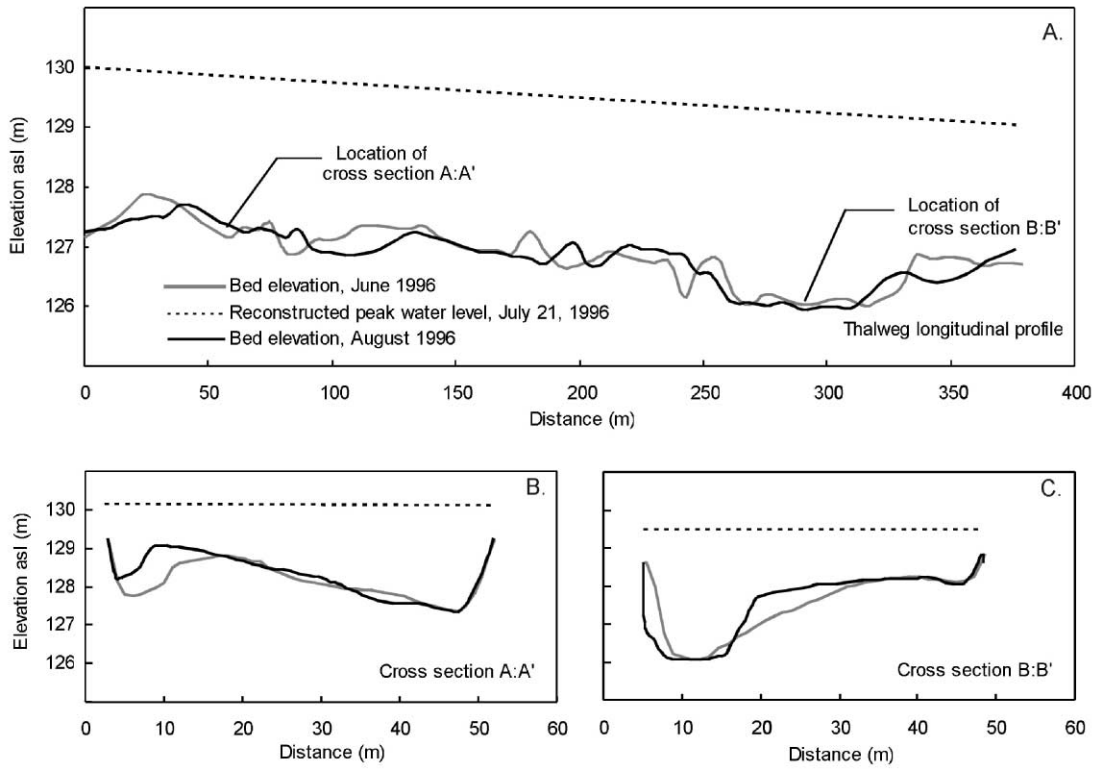

Fig. 8. Longitudinal (A) and cross-sectional (B and C) profiles of the study reach before and after the 275-year flood event. The cross-section locations are indicated in Fig. 4. The longitudinal profile follows the thalweg as shown on the July 1995 DEM. The reconstructed peak water elevation is shown on all profiles.

tween the left bank and bar 2 (at 230 m, Fig. 8A). Both bar 2 and bar 3 (Fig. 1) are unconstrained by bank protection and have migrated downstream more or less in unison, maintaining the diagonal riffle between them.

The overall finding is that the pattern of morphologic response between the two floods was qualitatively similar. Although the larger flood had multicentenary recurrence level and caused catastrophic morphologic change elsewhere in the region (Lapointe et al., 1998), the same types of adjustment occurred during both flood events, albeit at different rates.

5.2. Transport estimates based on morphologic methods

Using net volumetric changes in sediment storage calculated for 14 zones shown in Fig. 3, estimates of peak within-reach transport rates and average transport rates were calculated, they are presented in Table 2. A zero transport condition was specified at the upstream edge of zone 1 for the 7-year event and

Table 2
Sediment budget estimates of sediment transport[a]

Event	$I_b(dx, dy, dz)$ [kg event^{-1}]	$i_b(dx, dy, dz)$ [kg m^{-1} event^{-1}]	Zone[b]
Peak within-reach transport rate			
7-year	560,000	15,000	14
275-year	800,000	21,000	2
Average within-reach transport rate			
7-year	210,000	5600	
275-year	390,000	10,000	

[a] Estimates are reported to two significant figures only, reflecting the large uncertainties associated with all such estimates of transport.

[b] Peak within-reach transport rate is at the upstream boundary of this zone.

at the upstream edge of zone 14 for the 275-year event: transport rates in Table 2 are properly interpreted as a lower bound estimates.

Average $I_b(dx, dy, dz)$ for the 7-year flood was about half that of the 275-year flood (Table 2, bottom). However, peak $I_b(dx, dy, dz)$ for both events differ only by a factor of 1.5. As will be shown in Section 5.3, the expected difference based on fluid force alone would be by a factor of 5; this suggests that there was likely a large throughput component during the 275-year event, thereby causing a significant underestimation of $I_b(dx, dy, dz)$ for the 275-year event.

Estimates of the sediment transport based on the observed changes in morphology were also made for the 7-year flood event using the paired erosion/deposition zones approach: three paired erosion/deposition zones were identified. The three pairs and their inferred sediment transport vectors are shown in Fig. 5. For transport vectors I and III, discrete patches of net erosion or net deposition in close proximity (or destined for the same deposition location) were treated as a single erosion or deposition zone. The step length inferred for each pair, the estimated width of the bed over which sediment transport occurred, the volume of each individual patch, and the bulk sediment transport rate are presented in the first three columns of Table 3. Only transport vectors I and II represent transport occurring near the thalweg. Vector III is associated with the secondary channel behind bar 1. The values of $i_b(dx, dy, dz)$ calculated using the paired erosion/deposition approach for vectors I and II—1.7×10^4 kg m^{-1} event^{-1} and 1.4×10^4 kg m^{-1} event^{-1} (Table 3), respectively—are consistent with the analogous peak within-reach estimates calculated for the 7-year event using the sediment budget approach (1.5×10^4 kg m^{-1} event^{-1}) (Table 2). This suggests that the assumption of no net throughput is valid for the 7-year event. Given that the step length (80 m) is less than one quarter of the reach length (352 m), it is unlikely that bed material sediment arriving at the upstream boundary was transported past the downstream boundary during the 7-year event. Although patterns of erosion and deposition are similar for the 7- and 275-year floods, their volumes cannot be successfully matched for the 275-year event. The step length for this event almost certainly exceeded the reach length, so even if erosion/deposition pairs exist, our reach is too short to permit identification.

The simplicity of the paired erosion/deposition zone approach is appealing, but not all identifiable zones of erosion/deposition can be paired, which limits the applicability of this method. To generate more widely applicable estimates, the total erosion approach (Eq. (4)) was also used to calculate $I_b(dx, dy, dz)$. Step length was estimated for the 7-year flood to be approximately 80 m, using the results from the paired erosion/deposition approach. For the 275-year flood, a function relating the virtual transport rate (which represents the ratio of the step length to the duration of transport) to excess stream power (Hassan et al., 1992) was used to estimate step length. Based on the reach average stream power (Table 1), the virtual transport rate for the 275-year flood was 5.5 m h^{-1}; however, due to the large uncertainty associated with the stream power esti-

Table 3
Sediment transport estimates based on step length

Parameter	Paired erosion/deposition (7-year. event only)[a]			Total erosion	
	Vector I	Vector II	Vector III	7-Year event	275-Year event[b]
Step length (m)	82	86	64	80	542
Active channel width (m)	18	14	9	38	38
Erosion (m^3)	148 + 12	102	34 + 10	770	1437
Deposition (m^3)	168	107	38 + 7	N/A	N/A
i_b (kg m^{-1}event^{-1})	17,000	14,000	9200	8,700	110,000
I_b (kg event^{-1})	300,000	190,000	83,000	330,000	4,300,000

[a] See Fig. 5 for erosion/deposition pairs.

[b] The step length for this event was calculated using a function relating the virtual rate of transport to excess stream power (Hassan et al., 1992), and assuming that transport persisted for 4 days (per the analysis presented in Section 5.3).

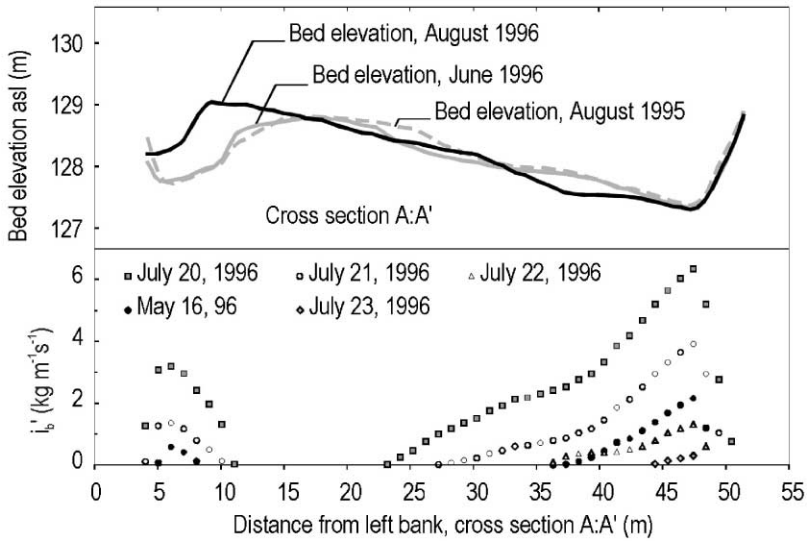

Fig. 9. The potential sediment transport field (assuming no pavement) at cross-section A–A′ is shown for May 16, 1996, and July 20–23, 1996. The bed elevations for all three survey periods are also shown. Note that the most significant morphologic change at this cross-section was the deposition occurring in the secondary channel along the left bank during the 275-year event.

mate, the virtual transport rate exhibits a wide range of values (1.88–10.8 m h^{-1}). Given that sediment transport is assumed to have occurred over 4 days (see Section 5.3), the step length for the 275-year event is an estimated 542 m. Total erosion estimates of $I_b(\mathrm{d}x, \mathrm{d}y, \mathrm{d}z)$ are presented in the fourth column of Table 3.

Reach average $I_b(\mathrm{d}x, \mathrm{d}y, \mathrm{d}z)$ was estimated to be 3.3×10^5 and 4.3×10^6 kg event^{-1} for the 7- and 275-year floods, respectively. The transport rate for the 7-year event is close to the corresponding sediment budget estimate (2.1×10^5 kg event^{-1}). The estimate for the 275-year flood (4.3×10^6 kg event^{-1}) is fully an order of magnitude larger than the 275-year sediment budget estimate (3.9×10^5 kg event^{-1}), and than all the 7-year event estimates. Even considering the range in the virtual transport rate, it is likely that the discrepancy in 275-year estimates reflects significant throughput of sediment that introduces a large negative bias to the sediment budget estimates.

5.3. Transport estimates using the dimensionless sediment transport ratio (q^*)

Cross-sectional profiles at section A–A′ from each survey are overlain in Fig. 9. Also shown is the estimated potential bed material transport field (i_b') calculated at 1-m intervals across the channel at cross-section A–A′ using the Meyer-Peter and Muller equation for May 16, 1996 and July 20–23, 1996. The estimate of I_b' for the 7- and 275-year events are presented in Table 4. Using the sedimentological data for bars 1, 2, and 3 and the reach-average shear stress estimates presented in Table 1, q^* was calculated for the 7- and 275-year peak flood conditions (Table 5). The values of q^* associated with the 7-year flood event indicate a relatively high rate of sediment supply to bar 1 from the complex point bars upstream (Fig. 1), despite the bank protection

Table 4
Potential sediment transport estimates based on flow conditions

Date	Potential sediment transport (I_b')		
	(kg s^{-1})	(kg day^{-1})	(kg event^{-1})
July 20, 1996	92	7,900,000	
July 21, 1996	38	3,300,000	
July 22, 1996	8.0	690,000	
July 23, 1996	0.67	58,000	12,000,000
May 16, 1996	13	1,100,000	2,200,000[a]

[a]While the event duration is unknown, the calculated virtual transport rate of 1.67 m h^{-1} (after Hassan et al., 1992) and the known step length of 80 m implies an event duration of 48 h.

Table 5
Dimensionless sediment transport ratio and associated sediment transport estimates

Event	Dimensionless sediment transport ratio (q^*)				$I_b(q^*, I'_b)$ [kg event^{-1}]
	Bar 1	Bar 2	Bar 3	Average	
7-year	0.60	0.00	0.10	0.23	520,000
275-year	0.74	0.27	0.24	0.42	5,000,000

measures located there. For bar 2, q^* is 0, reflecting the characteristic step length of about 80 m for this event and the restricted sediment supply to bar 2 from the riprap-protected cutbank upstream. The value of q^* increases at bar 3, reflecting the input of sediment from the eroding bank opposite bar 2. The values of q^* associated with the 275-year event reflect a similar trend. However, the higher flows have mobilized more sediment—either due to bank erosion or due to disruption of the armor layer—and transported it further. As a result, sediment transport is less supply limited during the 275-year event, but is still less than that predicted by the fluid force alone (that is $q^* < 1$ and $I_b < I'_b$).

By averaging q^* over the reach and applying the result to the I'_b estimates, values for $I_b(q^*, I'_b)$ have been calculated for the 7- and 275-year events. While the duration of sediment transport during the 7-year event is not known, observations by workers in the field suggest that transport likely persisted for between 1 and 2 days. Using the calculated virtual transport rate of 1.67 m h^{-1} (after Hassan et al., 1992), and the known step length of 80 m, the implied duration of transport is 48 h. Assuming a transport duration of 2 days, $I_b(q^*, I'_b)$ for the 7-year event was estimated to be 5.2×10^5 kg event^{-1}. This agrees well with all $I_b(\mathrm{d}x, \mathrm{d}y, \mathrm{d}z)$ estimates, especially considering these are lower bound estimates of the total bed material transport. The consistency of the $I_b(q^*, I'_b)$ estimates and the $I_b(\mathrm{d}x, \mathrm{d}y, \mathrm{d}z)$ estimates for the 7-year event provide some confidence in the use of the q^* and I'_b to calculate bed material transport rates.

The value of $I_b(q^*, I'_b)$ for the 275-year event is about 5.0×10^6 kg event^{-1} (Table 5), fully an order of magnitude larger than all estimates for the 7-year event. This closely matches the total erosion transport rate (4.3×10^6 kg event^{-1}). The sediment budget approach produces an average transport rate of only 3.9×10^5 kg event^{-1}, and a peak estimate that is not much higher, at 8.0×10^5 kg event^{-1} (Table 2).

6. Discussion

All of the morphologic methods work well when applied to the 7-year flood event. This is attributable to (i) the accuracy of the DEMs used to identify net erosion and deposition, and (ii) to the fact that the step length is much less than the reach length, which implies that little (if any) sediment throughput occurred. As a consequence, all methods give similar, and conceptually consistent results. Compensating scour and fill has not be addressed, and—while the effect of sediment throughput can be discounted for this event—substantial uncertainty in the actual transport rates for this event exist. However, we can confidently establish a lower bound for the reach average sediment transport $I_b(\mathrm{d}x, \mathrm{d}y, \mathrm{d}z)$ at 2.1×10^5 to 3.3×10^5 kg event^{-1}. Similarly, the peak within reach sediment transport $i_b(\mathrm{d}x, \mathrm{d}y, \mathrm{d}z)$ is known to be at least 1.4×10^4 to 1.7×10^5 kg event^{-1}.

Based on the fluid force, transport for the 7-year event is estimated to be 2.2×10^6 kg event^{-1} (I'_b). However, order of magnitude errors are common for fluid force-based equations (Gomez and Church, 1989), and we attribute much of the difference between I'_b and $I_b(\mathrm{d}x, \mathrm{d}y, \mathrm{d}z)$ to poor performance of the Meyer-Peter and Muller equation. When q^* is used to scale I'_b, the 7-year event sediment transport $I_b(I'_b, q^*)$ is estimated to be 5.2×10^5 kg event^{-1}. Given that $I_b(\mathrm{d}x, \mathrm{d}y, \mathrm{d}z)$ estimates are lower bounds, the $I_b(I'_b, q^*)$ transport rate corresponds very well. If we assume that $I_b(I'_b, q^*)$ represents the actual transport, and that the difference between $I_b(\mathrm{d}x, \mathrm{d}y, \mathrm{d}z)$ and $I_b(I'_b, q^*)$ is entirely attributed to compensating scour and fill, then a volume of (undetected) compensating scour and fill on the order 60% of the net erosion volume must have occurred. This is possible, and suggests that $I_b(I'_b, q^*)$ may closely represent the actual transport rate.

The good agreement between $I_b(\mathrm{d}x, \mathrm{d}y, \mathrm{d}z)$ and $I_b(I'_b, q^*)$ estimates suggests that fluid force-based

equations—which to date have not been notably successful in predicting sediment transport in rivers other than those for which they were developed—may be more generally applicable if the degree of sediment supply limitation is also accounted for. If this is in fact generally true, event-scale sediment transport could be estimated relatively easily, requiring only estimates of the flow conditions and the degree of bed surface armoring. This is an interesting topic that deserves further investigation.

Morphologic methods work less well for the 275-year event. Step length for this event was at least as large as the reach length, which introduces the problem of significant sediment throughput. As a result, only the total erosion approach was successfully implemented, and that required using the virtual transport rate (after Hassan et al., 1992) to estimate step length. However, the $I_b(\mathrm{d}x, \mathrm{d}y, \mathrm{d}z)$ estimate of 4.3×10^6 kg event^{-1} corresponds closely to the $I_b(I'_b, q^*)$ rate of 5.0×10^6 kg event^{-1}, which is encouraging. While large uncertainties (associated primarily with the estimated virtual transport velocity) preclude any definitive conclusions about the relative performance of these two sediment transport estimation methodologies, the results support the interpretations of the 7-year event estimates, and clearly indicate that transport rates during the 275-year event were an order of magnitude higher than those during the 7-year event.

Given this disparity in sediment transport rates, why did qualitatively similar patterns of channel adjustment persist in the face of such disparate transport magnitudes? Neither the two- or threefold channel widening nor the change in channel pattern observed by other researchers (Harvey, 1984; Nolan and Marron, 1985; Desloges and Church, 1992; Huckleberry, 1994; Warburton, 1994) have been observed on the Sainte Marguerite River after the 275-year flood. Others have reported similar apparent channel stability in the face of extreme flood events in eastern North America (Ritter, 1974; Gardner, 1977), but they had to rely on aerial photographs and isolated cross-sections to identify channel changes. Here, using the detailed pre and post-flood surveys of reach morphology, not only was the stability of the overall channel morphology demonstrated but also the relative stability of individual morphologic elements such as bars and pools.

Gardner (1977) attributes the observed channel stability in response to a 500-year flood event in Ontario to the river valley's geomorphically well-adjusted condition. That is, the river valley had experienced such rare flood events in the past and was adjusted so as to pass them without undue modification of the extant channel morphology. Gardner also notes that this well-adjusted condition is disturbed where man-made structures alter the nature of the channel and/or adjacent flood plain. Sainte Marguerite River may have been subject to floods of similar magnitude to the 275-year event in the recent geomorphic past and might have been geomorphically adapted to such events. However, the study reach is located near the upstream end of an 8-km section of river that was rectified and channelized nearly 40 year ago, and the newly channelized river cannot be adjusted to conditions existing prior to this recent manipulation.

The observed degree of stability may in part be attributed to the incidental effects of previous manipulation. Rectification increased the channel slope and thus the channel transport capacity. This in itself is similar to the effect of an extreme flood: both result in increases in stream power and shear stress, and both tend to straighten the river channel. The channelization has changed the channel morphology from a meandering system with a sinuosity of 1.9 that migrates primarily by meander extension and cut-off to a wandering gravel-bed river with a sinuosity of 1.2 that migrates by a combination of meander extension and lateral translation of alternate bars. This comprises a significant shift in channel regime. One may speculate that extreme floods would have tended to force the Sainte Marguerite River in its sinuous, unchannelized condition toward its current morphological condition, or even a braided condition, if sufficient sediment was input as a result of bank erosion. This is consistent with the previously reported concentration of the observed changes in other rivers at meander bends (Gardner, 1977).

Furthermore, the channelization has resulted in bed degradation of between 0.5 and 1.0 m in the vicinity of the study reach (Talbot and Lapointe, in review/a). The combination of bed degradation and reduced sinuosity likely dramatically reduced the depth of overbank flooding at the study reach. Based on cross-sections A–A′ and B–B′ and considering

the inferred peak water elevation shown in Fig. 8, overbank flow depths were likely at most 0.75 m, which—based on the water surface slope in the channel—infers an associated flood plain shear stress of approximately 20 N m^{-2}. This is far less than the critical value of 100 N m^{-2} identified as a threshold for forested flood plain erosion in general (Miller, 1990; Magilligan, 1992). A study of the effects of the July 20, 1996, event undertaken on the nearby Ha! Ha! River confirmed the applicability of this threshold value for the Saguenay region (Lapointe et al., 1998).

In addition to historic channelization, this part of the Sainte Marguerite River was subject in 1993 to extensive bank protection designed to reduce the rates of lateral channel migration. This bank protection remained intact during the 275-year flood and limited both the channel widening and the sediment supply. The riprap apparently restricted bar development during both floods, and has forced the bar to adjust to sediment supplied at the upstream end via a 'conveyor belt' style of scour and fill, rather than the typical pattern of persistent bar deposition and bank retreat. More extensive channel modification would likely have been observed—especially during the 275-year event—if the riprap had not been in place.

7. Conclusions

The morphologic methods applied in this study gave reasonable, consistent results. While the results were more consistent for the 7-year event than for the 275-year event, this does not imply that morphologic methods are not applicable to rare flood events. There are two criteria that likely determine where and when the various methods are applicable: (i) the step length relative to the reach length, and (ii) the step length relative to the bar-to-bar spacing.

When the step length is much less than the reach length (e.g., the 7-year event, for which step length = 80 m and reach length = 352 m), sediment throughput is small, and the sediment budget gives meaningful results. When the step length and reach length are of similar magnitude (e.g., the 275-year event, for which step length = 542 m), sediment throughput is significant, and introduces a large negative bias for the transport estimates. When the step length is less than the bar-to-bar spacing (typically found to be 5–7 channel widths), erosion and deposition pairs can be confidently identified because the transport vectors are easily deduced from the general flow structure in a bar–riffle–pool sequence. When the step length exceeds the bar to bar spacing (as it does for the 275-year event studied here), it becomes much more difficult to unambiguously identify erosion and deposition pairs because the step lengths now involve complex transport paths that may be significantly affected by local flow structure. Therefore, the pair erosion/deposition approach may well not be applicable to large flood events. Neither of these two constraints affect the total erosion method, provided a reasonable step length can be estimated.

Bed material transport can also be calculated using a fluid force equation (here the well known Meyer-Peter and Muller equation) and some index of the event-scale sediment supply (here q^* presented by Dietrich et al., 1989). Our findings show that this approach gives reasonable results for two very different transport rates, and it is conceptually well grounded. While the results so far are very promising, further testing of this approach against other bed material transport data sets should reveal if it is generally applicable.

Morphologic stability can persist—even when transport rates are exceptionally high and step lengths exceed the scale of bar–riffle–pool spacing—when the stream channel has been conditioned by previous channel modification. The modification can be natural (e.g., Gardner, 1977) or anthropogenic. The 275-year flood studied here did not qualitatively alter the channel pattern nor did it cause extensive modification of the existing morphologic elements. Such channel stability is attributable to the recent human alteration (straightening and incision), which represents a change in channel pattern and has altered the interaction between the river and its flood plain. It has conditioned this reach of the Sainte Marguerite River in such a way that it is able to pass an extreme event (such as the 275-year flood) without significantly altering its morphology.

Acknowledgements

This paper is part of the scientific program of CIRSA, the Centre Interuniversitaire de Recherche

sur le Saumon Atlantique. Dr. M. Church provided comments on an early draft of this paper, which helped develop the ideas presented herein. Review comments provided by Dr. R.A. Marston and Dr. B. Bauer helped to improve this paper. Review comments provided by Dr. P. Ashmore were particularly useful, and led to a significant improvement of the paper. Dr. M. Hassan also provided helpful guidance in the final stages of preparing this work. Field work was completed with help from field assistants working at the CIRSA camp during the summers of 1995 and 1996. We are especially grateful for the outstanding contributions made in the field by Cindy Honeywill, Steve Driscoll and Nicole Couture.

References

Ashmore, P.E., Church, M., 1998. Sediment transport and river morphology: a paradigm for study. In: Klingeman, P.C., Beschta, R.L., Komar, P.D., Bradley, J.B. (Eds.), Gravel-bed Rivers in the Environment. Water Resources Publications, Colorado, pp. 115–148.

Carling, P.A., Reader, N.A., 1982. Structure, composition and bulk properties of upland streams and gravels. Earth Surf. Processes Landforms 7, 349–365.

Carson, M.A., Griffiths, G.A., 1987. Bedload transport in gravel channels. J. Hydrol. (NZ) 26, 1–151.

Carson, M.A., Griffiths, G.A., 1989. Gravel transport in the braided Waimakariri River: mechanisms, measurements and predictions. J. Hydrol. 109, 201–220.

Church, M., McLean, D.G., Wolcott, J.F., 1987. River bed gravels: sampling and analysis. In: Thorne, C.R., Bathurst, J.C., Hey, R.D. (Eds.), Sediment Transport in Gravel-Bed Rivers. Wiley, New York, NY, pp. 43–88.

Church, M., Hassan, M.A., Wolcott, J.F., 1998. Stabilizing self-organized structures in gravel-bed stream channels: field and experimental observations. Water Resour. Res. 34 (11), 3169–3179.

Desloges, J.R., Church, M., 1992. Geomorphic implications of glacier outburst flooding: Noeick River valley, British Columbia. Can. J. Earth Sci. 29, 551–564.

Dietrich, W.E., Kirchner, J.W., Ikeda, H., Iseya, F., 1989. Sediment supply and the development of the coarse surface layer in gravel-bedded rivers. Nature 340, 215–216.

Eaton, B.C., 1996. Morphologic channel response to flood events in a salmon spawning stream. MS Thesis, McGill University, Montreal.

Gardner, J.S., 1977. Some geomorphic effects of a catastrophic flood on the Grand River, Ontario. Can. J. Earth Sci. 14, 2294–2300.

Goff, J.R., Ashmore, P.E., 1994. Gravel transport and morphological change in braided Sunwapta River, Alberta, Canada. Earth Surf. Processes Landforms 19, 195–212.

Gomez, B., Church, M., 1989. An assessment of bed load sediment transport formulae for gravel bed rivers. Water Resour. Res. 25 (6), 1161–1186.

Graton, L.C., Fraser, H.J., 1935. Systematic packing of spheres with particular relation to porosity and permeability. J. Geol. 43, 785–909.

Ham, D.G., Church, M., 2000. Bed-material transport estimated from channel morphodynamics: Chilliwack River, British Columbia. Earth Surf. Processes Landforms 25, 1123–1142.

Harvey, A.M., 1984. Geomorphological response to an extreme flood: a case from southeast Spain. Earth Surf. Processes Landforms 9, 267–279.

Haschenburger, J.K., Church, M., 1998. Bed material transport estimated from the virtual velocity of sediment. Earth Surf. Processes Landforms 23, 791–808.

Hassan, M., 1990. Scour, fill and burial depth of coarse material in gravel bed streams. Earth Surf. Processes Landforms 15, 341–356.

Hassan, M., Church, M., Ashworth, P.J., 1992. Virtual rate and mean distance of travel of individual clasts in gravel-bed channels. Earth Surf. Processes Landforms 17, 617–627.

Hubbel, D.W., 1964. Apparatus and techniques for measuring bed load. U.S. Geol. Surv. Water-Supply Pap. 1748, 74 pp.

Huckleberry, G., 1994. Contrasting channel response to floods on the middle Gila River, Arizona. Geology 22, 1083–1086.

Lane, S.N., Richards, K.S., Chandler, J.H., 1995. Morphological estimation of the time-integrated bed load transport rate. Water Resour. Res. 31 (3), 761–772.

Lapointe, M.F., Secretan, Y., Driscoll, S.N., Bergeron, N., Leclerc, M., 1998. Response of the Ha! Ha! River to the flood of July 1996 in the Saguenay Region of Quebec: large-scale avulsion in a glaciated valley. Water Resour. Res. 34 (9), 2383–2392.

Magilligan, F.J., 1992. Thresholds and the spatial variability of flood power during extreme floods. Geomorphology 5, 373–390.

Martin, Y., Church, M., 1995. Bed-material transport estimated from channel surveys: Vedder River, British Columbia. Earth Surf. Processes Landforms 20, 347–361.

Miller, A.J., 1990. Flood hydrology and geomorphic effectiveness in the Central Appalachians. Earth Surf. Processes Landforms 15, 119–134.

Neill, C.R., 1971. River bed transport related to meander migration rate. J. Waterw., Harbors Coastal Eng. Div., Am. Soc. Civ. Eng. 97, 783–786.

Neill, C.R., 1987. Sediment balance considerations linking long-term transport and channel process. In: Thorne, C.R., Bathurst, J.C., Hey, R.D. (Eds.), Sediment Transport in Gravel-bed Rivers. Wiley, New York, NY, pp. 225–240.

Nolan, K.M., Marron, D.C., 1985. Contrast in stream-channel response to major storms in two mountainous areas of California. Geology 13, 135–138.

Popov, I.V., 1962. A sediment balance of river reaches and its use for the characteristics of the channel process. Trans. State Hydrol. Inst. 94, 3–21 Translated in Soviet Hydrology (1962) 249–267.

Reid, I., Frostick, L.E., 1994. Fluvial sediment transport and deposition. In: Pye, K. (Ed.), Sediment Transport and Depositional Processes. Blackwell, Cambridge, MA, pp. 89–192.

Ritter, J.R., 1974. The effects of the hurricane Agnes flood on channel geometry and sediment discharge of selected streams in the Susquehanna River basin, Pennsylvania. U.S. Geol. Surv. J. Res. 2 (6), 753–761.

Talbot, T., Lapointe, M.F., in review/a. The multiple responses of a gravel bed river to large-scale meander rectification: the case of the Sainte-Marguerite River, Saguenay Region, Quebec. Submitted to Water Resour. Res.

Talbot, T., Lapointe., M., in review/b. Numerical modelling of gravel bed river response to large-scale meander rectification: the coupling between the evolutions of bed pavement and long profile. Submitted to Water Resour. Res.

Warburton, J., 1994. Channel change in relation to meltwater flooding, Bas Glacier d'Arolla, Switzerland. Geomorphology 11, 141–149.

Wathen, S.J., Hoey, T.B., 1998. Morphological controls on the downstream passage of a sediment wave in a gravel-bed stream. Earth Surf. Processes Landforms 23, 715–730.